Proceedings of ERAD 2006

Spectral Polarimetric VAD separates bird from insect (wind) velocities

Svetlana Bachmann[1,2], Dusan Zrnic[2]

[1] University of Oklahoma, Norman (USA).

[2] National Severe Strom Laboratory, Norman (USA).

1 Introduction

With the current signal processor on the WSR-88D network radar moments can be computed in the frequency domain, as opposed to the generally accepted time domain computations. Although the frequency domain estimation is more computationally complex, it offers great possibility for clutter filtering, noise removing, and signal enhancing techniques as well as signal content exploration. Because of the size of the radar resolution volume, different scatterers might contribute to the resultant value of the estimated radar moments, such as velocity, reflectivity, etc. In a clear air case the combination contributing to the radar moments can include echoes from water particles, refractive index fluctuation, grass debris, insects, birds, aircrafts, radio interference, and ground targets. Spectral clutter filtering techniques and point target notch filters are being accepted and used in several radar applications. The task of separating migrating birds and insects is more challenging. We demonstrate a spectral processing technique that allows discrimination of birds and insect mixed within each resolution volume over a large area. This case occurred on the evening of September 7, 2004, during the beginning of bird migration season over the Great Plains in the USA. We use polarimetric spectral densities to identify and discriminate the scatterer types. Spectral densities of polarimetric variables are used to construct spectral azimuth displays (spectral VAD). Analyses of the spectral VADs reveal the mean velocities and the directions of the two types of scatterers.

Correspondence to: Svetlana Bachmann

svetlana.bachmann@noaa.gov

2 Radar data and weather conditions

Time-series data were collected with the NOAA/NSSL research S-band radar (KOUN) on September 7, 2004 at 11 pm local time (04 UT). Radar was in dual polarization mode, simultaneously transmitting and receiving waves of horizontal (H) and vertical (V) polarizations. The pulse repetition time was 780 μs and the number of samples M for spectral analysis was 128. Consequently the unambiguous range R_a and velocity v_a were 117 km and 35 m s^{-1}. Fair weather and a north-northeast wind at 5 to 10 m s^{-1} were recorded on this day. However, the velocities registered by the radar reach 30 m s^{-1} (Fig.8a). Radar meteorologists attribute this inconsistency to "contamination by biological scatterers" and discard such data as worthless for meteorological interpretation. We demonstrate that spectral analysis and polarimetry can be used to retrieve both the winds and the bird speeds in this and similar situations.

3 Polarimetric spectral densities

Power spectral density (PSD) is estimated from the time series data weighted with the von Hann window for each channel of the dual polarization weather radar, producing two PSDs in H and V polarizations. The differential properties at localized, resolved Doppler shifts are estimated directly from the spectral coefficients of the two PSDs. For M transmitted pulses there are M spectral coefficients from a resolution volume. Let k be an ordered number of spectral coefficient that takes values from 1 to M; k can be transformed to its corresponding radial velocity in the unambiguous velocity interval from $-v_a$ to v_a. Then, $s_h(k)$ and $s_v(k)$ are an H-V pair of complex spectral coefficients containing both the signal and the noise from the corresponding channels. To obtain spectral densities of differential reflectivity, the Z_{DR} values are computed for every H-V pair of spectral coefficients of the power spectral

densities similar to Kezys et al. (1993), and Yanovsky et al. (2005) according to

$$Z_{DR}(k) = 10\log_{10}\frac{|s_h(k)|^2}{|s_v(k)|^2} + C, \text{(dB)}, \qquad (1)$$

where C is the calibration constant that accounts for the difference in the system gains of the two channels. We estimate the spectral densities of the complex copolar correlation coefficient (magnitude and phase) from a running 3-point average on contiguous complex spectral coefficients of the H and V channels

$$\rho_{hv}(k) = \frac{\sum_{m=<k-1>_M}^{<k+1>_M} s_h(m)s_v{}^*(m)}{\sqrt{\sum_{m=<k-1>_M}^{<k+1>_M}|s_h(m)|^2 \sum_{m=<k-1>_M}^{<k+1>_M}|s_v(m)|^2}} \qquad (2)$$

The spectral density of the differential phase is computed relative to the system phase. We estimated the system phase of the KOUN digital receiver from the ground clutter reflectivity returns according to Zrnic et al. (2005).

4 Spectral densities along range

Doppler power spectral densities are presented as a function of radial velocity. The PSD plots (Fig.1) show power in $\log_{10}$ relative units. One column in the image at some range R represents the spectrum at that range. In the presence of scatterers the image is expected to display a somewhat continuous distinct band corresponding to the radial component of the scatterers' velocities. Thus, in an ideal case this band represents the dependence of radial velocities on range that should be consistent with the sounding wind profile. Other curves and blobs, which deviate from the band tracing the mean wind, are contaminants, as documented by Bachmann and Zrnic (2005). The appearance and explanation are analogues to the case of wind profiling radars (Cornman et al. 1998), whereby clear-air spectra are often contaminated by birds or ground clutter. Spectral densities of polarimetric variables (ρ_{hv}, Z_{DR} and δ) along the radial are shown in Fig. 2a, 2b, and 2c.

The mean noise level in spectra can be estimated and used to remove the spectral coefficients from the spectral densities of polarimetric variable fields (Fig.3). Two distinctive bands can be observed in Fig. 1, 2, and 3. A continuous band and a sporadic band are located at velocities of about 10 and 20 m s^{-1} respectively. The bands are clearly separated in velocity. The polarimetric properties, shapes of the bands, and the values of the associated velocities reveal that insects and birds shared the airspace throughout most of the boundary layer on that night (Bachmann and Zrnic 2005). The band from the insects exhibits higher values of Z_{DR} (3 dB<Z_{DR}<10 dB), higher values of ρ_{hv} (0.8<ρ_{hv}<1), and a narrow range of phases (50°<δ< 80°). The band from birds shows smaller values of Z_{DR} (Z_{DR}<3), smaller values in the mean of ρ_{hv} (ρ_{hv}~0.7), and all possible phases (-180°<δ<180°). Each spectral field (Fig.1, 2, and 3) exhibits a well defined band

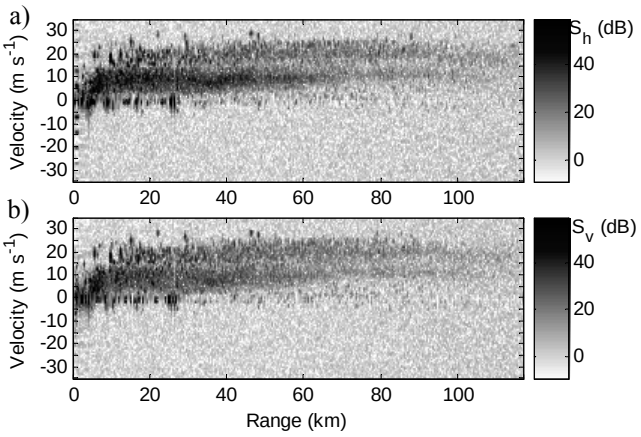

Fig. 1. Field of PSD a) in H, b) in V channel.

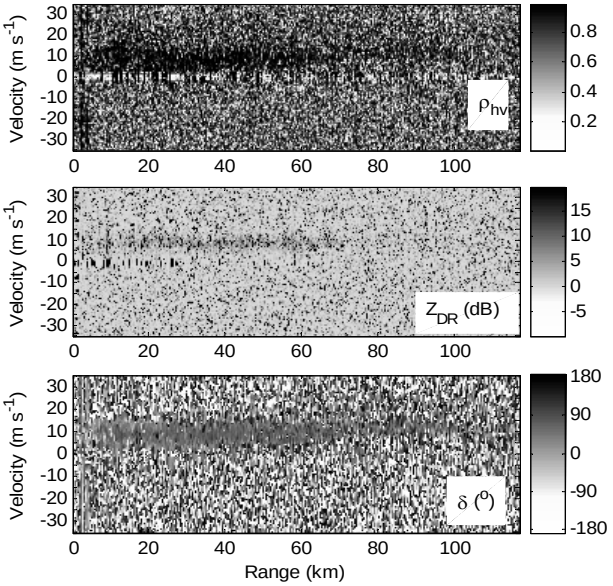

Fig. 2. Spectral densities of a)ρ_{hv}, b) Z_{DR} and c) δ.

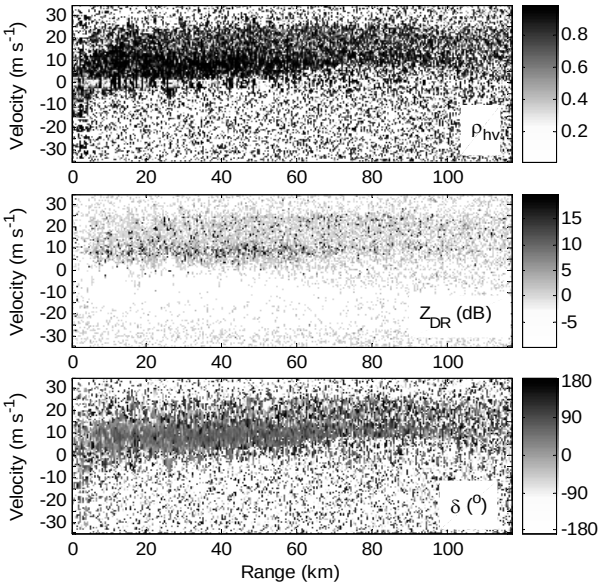

Fig. 3. Spectral densities of a)ρ_{hv}, b) Z_{DR} and c) δ after a power threshold.

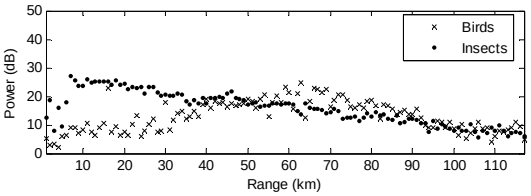

Fig. 4. Power in spectral coefficients of the bird and insect bands. Average power for azimuths from 178 to 182 degrees.

(from insects) that stretches to 70 km in range and than dissipates due to low signal. The maximum powers in the bands can be estimated from the spectral peaks (Fig.4). The return power in the insect band decreases with range, while the power in the bird band has a peak at about 60 km indicating that birds tend to form a layer.

5 Spectral density fields in azimuth

The velocity azimuth display (VAD) technique, developed by Rabin and Zrnic (1979), is part of a suite of algorithms on the WSR-88D and is used to determine several features of the wind field: aerial average wind speed, direction, divergence and deformation (Doviak and Zrnic 1983, Rabin and Zrnic 1979). The spectral VAD (SVAD) displays the distributions of velocities with associated powers and polarimetric properties in azimuth.

Fig.5a shows SVAD of power S_h composed for the one range location at 30 km. A sinusoidal trace with a broad spectrum width (up to 20 m s^{-1}) demonstrates the severe contamination by birds.

Fig.5b shows SVAD for a median over a 40 km range interval (from 30 to 70 km) i.e., a total 120 spectra are averaged to enhance visual clarity. Two traces are clearly seen and both have sinusoidal shapes. The two sinusoids in the S_h-SVAD indicate 12 m s^{-1} from North-East to South-West; and 20 m s^{-1} from North to South. The polarimetric properties of these sinusoids are different (not shown). In the Z_{DR}-SVAD the sinusoid with smaller amplitude appears bright and well defined with 5 to 8 dB values corresponding to the insect returns. However, the sinusoid with larger amplitude has smaller Z_{DR} values. This sinusoid is due to returns from birds. At the regions where the two sinusoids intersect (at 60 degrees and 240 degrees) there is a lowering of the insect Z_{DR} due to the mixture of both scatterer types.

Fig.6 show SVAD ensemble (S_h, Z_{DR}, ρ_{hv}, and δ) composed of a median of spectral densities from 30 to 35 km; values above the noise level are displayed. The type of the variable is indicated above the colorbar of each SVAD. The median of spectral densities over 5 km almost completely removes the contribution from the birds.

The example presented in Fig. 7 illustrates construction of a VAD from the SVAD of Z_{DR} for a 5 km median (Fig.7a). The Z_{DR} spectral fields were modified (Fig.7b) as follows: all Z_{DR} spectral coefficients with the power below noise level and ρ_{hv} below 0.7 were removed; further, adaptive threshold was applied to remove all spectral coefficients of Z_{DR} below

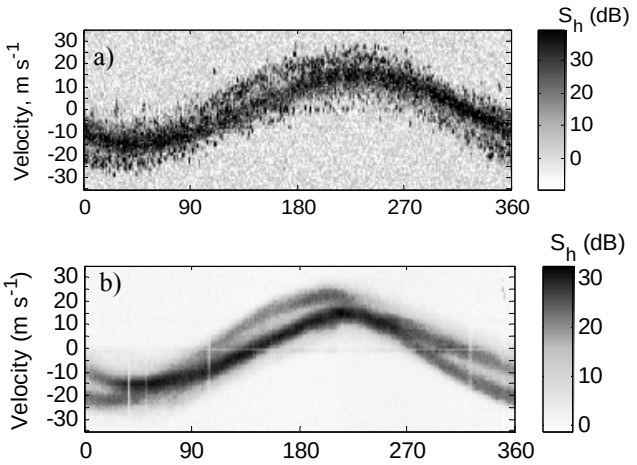

Fig. 5. The S_h-SVAD constructed for a) 30 km range, b) median of power spectral densities at ranges from 30 to 70 km.

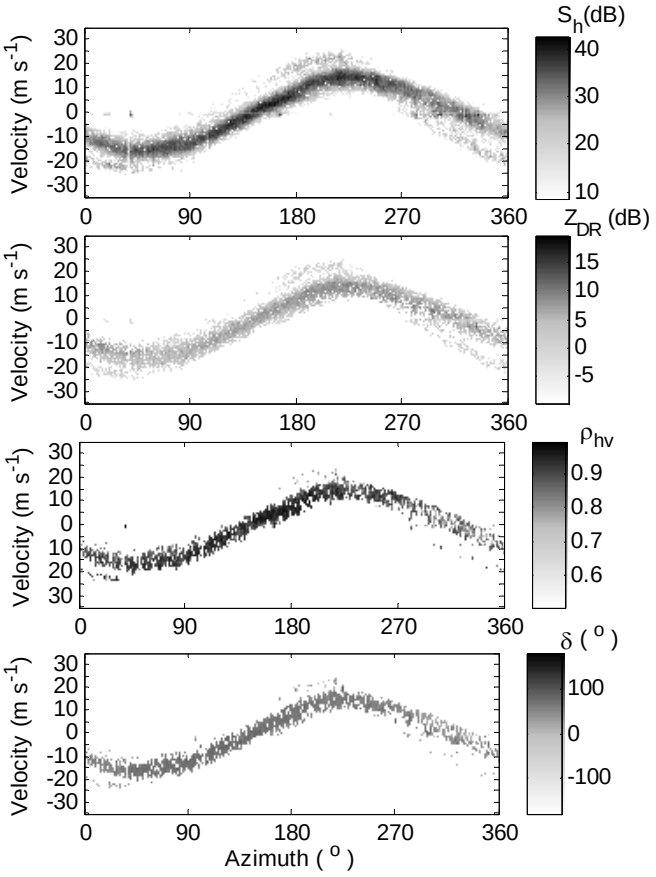

Fig. 6. The spectral VAD ensemble (S_h, Z_{DR}, ρ_{hv}, and δ) contracted for a median of spectral densities from 30 to 35 km.

half the maximum of the median value at the specified velocity bin; median filter over 3 range locations and 6 spectral coefficients was applied to smooth the gaps in the spectral densities; then, all spectral coefficients with Z_{DR} values below 2 dB were removed. Maximum value of Z_{DR} is chosen at every azimuth and its corresponding velocity is recorded for subsequent VAD processing (Fig.7c). The cross marker indicates the recorded velocities. The dashed line with a dot marker shows VAD estimated from two harmonics fit (DC and first).

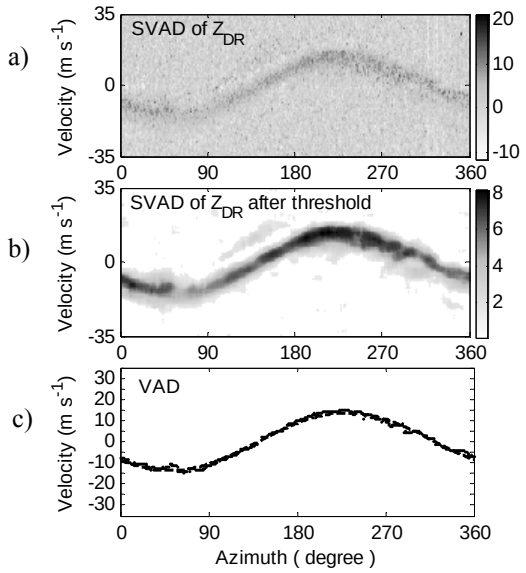

Fig. 7. VAD from Z_{DR} SVAD: a) Z_{DR} SVAD from average of spectral densities at ranges 30 to 35 km; b) Z_{DR} SVAD after thresholds; c) VAD.

From an ensemble of spectral VADs, the directions and velocities of insects and birds are deduced. If insects indeed are the wind tracers then the recovered wind velocity is shown in Fig.8b. The wind blows toward South West at 12 m s^{-1}. Birds fly South at 20 m s^{-1} (Bachmann and Zrnić, 2005).

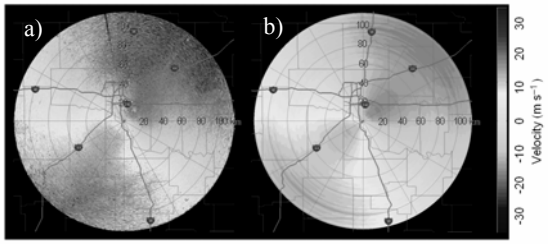

Fig. 8. Velocity a) contaminated, and b) recovered.

6 Conclusion

Spectral analyses of returns in clear air and at night reveal simultaneous presence of migrating birds and wind-blown insects throughout the boundary layer. The polarimetric variables (return power, differential reflectivity, copolar correlation coefficient, and differential phase) associated with resolvable Doppler shifts are computed from the Doppler spectra of horizontally and vertically polarized returns. Thus the spectral density of these polarimetric variables exhibit separation of the two species.

We demonstrate that the speed measurements of insects and migrating birds can be resolved by constructing spectral VADs and isolating the insect velocity sinusoid from the additional sinusoids caused by contaminants such as birds. Further from the combined use of the spectral densities of the polarimetric variables, it might be possible to reconstruct velocity azimuth (VAD) profiles of the wind. Specifically we use the copolar correlation coefficient and the signal to noise ratio to isolate the spectral values of Z_{DR} which are caused by insects. Then we associate the velocity at the maximum value of such thresholded Z_{DR} spectra with the return from insects and perform a VAD analysis on these velocities. Spatial continuity and general agreement with winds measured by rawinsondes add credibility to our analysis.

Acknowledgements: Part of this work was supported by the National Weather Service, the Federal Aviation Administration, and the Air Force Weather Service through the NEXRAD Product Improvement Program. For the first author funding was provided by NOAA/Office of Oceanic and Atmospheric Research under NOAA-University of Oklahoma Cooperative Agreement #NA17RJ1227, U.S. Department of Commerce.

References

Bachmann, S. M., and D. S. Zrnic, 2005: Spectral polarimetry for identifying and separating mixed biological scatterers. Proceedings of, *32nd Int. Conf. on Radar Meteorology*, Albuquerque, NM, Amer. Meteor. Soc., P9R-5.

Cornman, L.B, R.K. Goodrich, C.S. Morse, and W.L. Ecklund, 1998: A fuzzy logic method for improved moment estimation from Doppler spectra. *J. Atmos. Oceanic Technol.*, **31,** 1287-1305.

Doviak R. J., and D. S. Zrnić, 1984: Doppler Radar and Weather Observations. *Academic Press*, 458 pp

Kezys, V., E. Torlaschi, and S. Haykin, 1993: Potential capabilities of coherent dual polarization X-band radar. Preprints, 26th Int. Conf. on Radar Meteorology, Norman, OK, Amer. Meteor. Soc., 106-108.

Rabin, R. M. and D. S. Zrnić, 1979: Subsynoptic Scale Vertical Wind Revealed by Dual Doppler Radar and VAD Analysis. *J. Atmos Sciences*, **37**, 644-654.

Yanovsky, F.J., H.W.J. Russchenberg, and C.M.H. Unal, 2005: Retrieval of information about turbulence in rain by using Doppler-polarimetric Radar. *IEEE Trans. Microw. Theory Tech.*, **53,** 444- 450.

Zrnic D. S., V. Melnikov, and J. K. Carter, 2005: Calibrating the differential reflectivity on WSR-88D. Proceedings of, *32nd Int. Conf. on Radar Meteorology*, Albuquerque, NM, Amer. Meteor. Soc., 4R-1